Nonlinear Science 7 (2026) 100128

Contents lists available at ScienceDirect

Nonlinear Science

journal homepage: www.elsevier.com/locate/nls

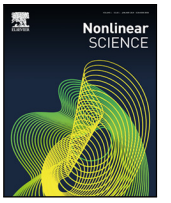

Research paper

Exact solutions for classes of nonlinear differential equations on fractal supports

Donatella Bongiorno [a,*], Alireza Khalili Golmankhaneh [b]

[a] Dipartimento di Ingegneria, Università di Palermo, Viale delle Scienze, Ed. 8, 90128 Palermo, Italy
[b] Department of Physics, Ur. C., Islamic Azad University, Urmia 63896, Iran

ARTICLE INFO

MSC:
28A80
34A30

Keywords:
Fractal set
Exact solution
Non linear fractal differential equations
Riccati-type fractal differential equations

ABSTRACT

In this paper, the exact solutions of certain non-linear differential equations defined on a fractal subset of the real line are presented. Particular attention is paid to the Riccati-type fractal differential equation, for which a connection with the Schrödinger equation is also provided. To further substantiate the theoretical findings, numerical validations are included, comparing the exact analytical solutions with results obtained through a generalized Fractal Euler Method.

1. Introduction

The study of non-linear differential equations (NDE) is a cornerstone of mathematical physics and engineering, providing essential models for complex phenomena across numerous disciplines, from fluid dynamics and quantum mechanics to biology and finance [1–3]. It is known that powerful analytical and numerical techniques exist for NDEs defined on standard Euclidean domains. Among the non-linear ordinary differential equations, the Riccati differential equation is a notable example. This equation, with quadratic right-hand sides, is closely linked to the calculus of variations and optimal control theory, playing a key role in the optimal control of complex networks [4–6]. Despite these advances, a significant challenge arises when the underlying domain possesses a non-integer, or fractal, dimension. This challenge is central given the relevance of fractal geometry in modeling and understanding natural phenomena (such as blood vessels, coastlines, mountains, and clouds) as highlighted in the classic exposition by B. Mandelbrot [7]. These fractal structures exhibit unique features, including self-similarity and fractal dimensions greater than their topological dimensions, which distinguish them from traditional Euclidean objects. Consequently, conventional metrics (e.g., length, surface area, and volume) typically applied to Euclidean forms have proven insufficient for analyzing the properties of analytic functions defined on a fractal set or on a fractal curve [8–10]. To address this, mathematical methods extending beyond classical analysis, such as harmonic analysis [11–13], measure theory [14,15], stochastic processes [16] and fractional calculus [17], were developed. In particular, fractional calculus has found extensive applications in analyzing the stability of complex systems such as neural networks [18,19]. Specifically, a method known as fractal calculus (F^α-calculus) was formulated for fractal subsets of the real line [20] and fractal curves [21], offering a framework highly similar to the classical one. In this paper, we adopt the F^α-calculus framework, initially introduced in [20] and later refined by A.K.G. in [22]. The parameter α, denoting the fractal dimension, is proven to coincide with the well-known Hausdorff dimension when the fractal set F is compact. Central to this formulation is the staircase function, which generalizes the Cantor staircase function and is the key to defining the fractal integral and derivative. The application of such calculus has led to significant recent progress, including the development of new methods for solving fractal

* Corresponding author.
E-mail addresses: donatella.bongiorno@unipa.it (D. Bongiorno), alireza.khalili@iau.ac.ir (A.K. Golmankhaneh).

https://doi.org/10.1016/j.nls.2026.100128
Received 25 October 2025; Received in revised form 1 March 2026; Accepted 21 March 2026
Available online 23 March 2026

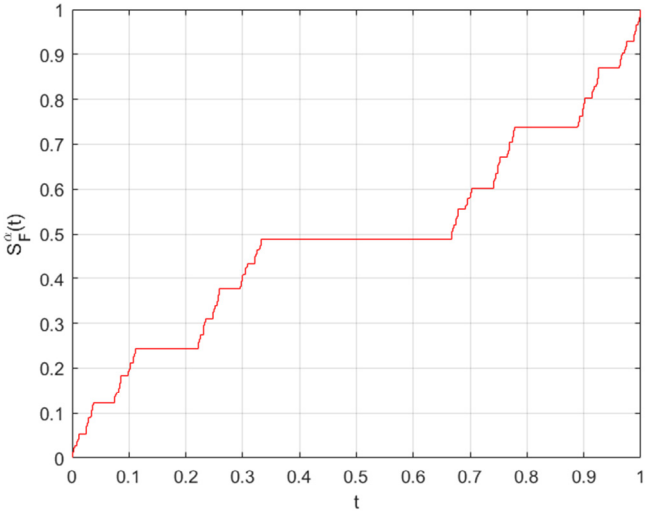

Fig. 1. Graphical representation of the Staircase function $S_F^\alpha(t)$ associated with the standard ternary Cantor set, here denoted by F. The figure illustrates the fundamental concepts of fractal calculus: the fractal set F corresponds to the points on the t-axis where the function increases, while the flat regions (plateaus) correspond to the gaps (complementary intervals) of F. Furthermore, $S_F^\alpha(t)$ serves as a canonical example of an F-continuous function.

differential equations (FDEs) [23,24] and systems of FDEs [25,26]. These models have proven effective in simulating processes with memory and modeling of fractal integral equations via Volterra fractal operator [27].

In this paper, we show how the F^α-calculus offers new avenues for finding exact solutions to some types of non-linear FDEs on fractal supports. The manuscript is organized as follows. Section 2 prepares the reader by reiterating and adapting crucial definitions derived from the work of A. Parvate and A. D. Gangal [20], tailoring them to our specific computational environment. The accompanying remarks highlight the mechanism by which fractal calculus extends the concepts of ordinary calculus, complemented by figures depicting their primary aspects. A definition of fractal-primitive and its characterization is also provided. In Section 3 we focus on the resolution of non-linear fractal differential equations of the form $D_F^\alpha y(t) = g(\phi(y,t))$, where g is an F-continuous function on a fractal set F and $\phi(y,t)$ is a given function. We demonstrate that specific changes of variables can reduce these complex problems into tractable linear FDEs with separable variables. Section 4 addresses the Riccati-type fractal differential equations (RFDE). Here, we analyze the equation and present three distinct analytical strategies for its resolution, which involve converting the RFDE into a Bernoulli-type equation through a known particular solution, transforming it into a first-order linear FDE to facilitate a faster solution process, or mapping the RFDE onto a second-order linear FDE. Additionally, we provide numerical validation using a generalized Fractal Euler Method to demonstrate the stability and robustness of these analytical solutions on the Cantor set.

In Section 5, we explore the physical implications of our findings by connecting the RFDE to the Schrödinger equation on fractal domains. By employing the factorization approach, we demonstrate how the superpotential of quantum systems, such as the fractal harmonic oscillator and the fractal Coulomb potential, satisfies a Riccati-type fractal differential equation.

Finally, Section 6 concludes the paper by summarizing the findings and suggesting directions for future research.

A Technical Appendix has been added at the end of the manuscript to improve legibility and comprehension.

2. Preliminary

In this section, we provide a brief overview of F^α-calculus, based on some definitions given in [20] and in [22], here suitably restated. Throughout all the paper we denote by F a compact α-perfect fractal subset of the real line, where $\alpha \in (0,1]$ is its fractal dimension. Moreover denoted by $[a,b]$ an interval of the real line, we assume that $F \cap [a,b] \neq \emptyset$.

Definition 1. Let $0 < \alpha \leq 1$. The *α-dimensional Hausdorff measure* of a subset A of the real line is defined as:

$$\mathcal{H}^\alpha(A) = \lim_{\delta \to 0} \inf \left\{ \sum_{i=1}^{\infty} (\mathrm{diam}(A_i))^\alpha \,:\, A \subset \bigcup_{i=1}^{\infty} A_i,\ \mathrm{diam}(A_i) \leq \delta \right\}.$$

Moreover, the unique number α for which $\mathcal{H}^t(A) = 0$ if $t > \alpha$ and $\mathcal{H}^t(A) = \infty$ if $t < \alpha$ is called the fractal (Hausdorff) dimension of A.

Definition 2. Let $[a,b]$ be an interval of the real line and let $t \in F \cap [a,b]$. The staircase function associated with the fractal set F of order α is defined by

$$S_F^{\alpha}(t) = \begin{cases} \Gamma(\alpha+1)\mathcal{H}^{\alpha}(F \cap [p,t]), & \text{if } t \geq p \\ -\Gamma(\alpha+1)\mathcal{H}^{\alpha}(F \cap [t,p]) & \text{if } t < p. \end{cases}$$

where $p \in [a,b]$ is fixed and $\Gamma(\cdot)$ is the well known gamma function.

Remark 2.1. The theoretical framework developed in this paper applies to a broad class of fractal sets F, such as the generalized Cantor sets $C(\lambda)$ (see [28]). To ensure clarity and illustrative consistency, most graphical representations and numerical experiments assume that F is the standard ternary Cantor set C (with $[a,b] = [0,1]$ and $p = 0$). Note that the staircase function associated with the standard ternary Cantor set C is depicted in Fig. 1. However, where explicitly stated (e.g., to analyze the sensitivity of the solution to the fractal support), we also employ generalized Cantor sets with different fractal dimensions (such as $\alpha = 0.5$, corresponding to a dissection ratio of $1/4$).

Definition 3. Let $[a,b]$ be an interval of the real line. Let $t \in F \cap [a,b]$ and let $r \in \mathbb{R}^+$. A fractal neighborhood with center t and radius r is the fractal interval of the form $V_F(t,r) = (t-r, t+r) \cap (F \cap [a,b])$.

Definition 4. Let $f : [a,b] \to \mathbb{R}$. We say that the function f is F-continuous at a point $t \in F \cap [a,b]$, if for every fractal neighborhood V_F of $f(t)$ there exists a fractal neighborhood W_F of t such that $f(t) \in V_F$ whenever $t \in W_F$. In other words f is F-continuous at a point $t \in F$ if the following fractal limit exists

$$F\text{-}\lim_{y \to t} f(y) = f(t).$$

Whenever f is F-continuous at every point of $F \cap [a,b]$, then f is called a F-continuous function. The set of all such functions is denoted by $C(F \cap [a,b])$.

Remark 2.2. Note that the previous definition does not involve values of the function f at a point y if $y \notin F \cap [a,b]$. Therefore, the notion of F-continuity is a generalization of the classical notion of continuity. An example of a F-continuous function can be found in Fig. 1 .

Definition 5.

Let $f : [a,b] \to \mathbb{R}$. The fractal derivative of a function f at a point $t \in [a,b]$ is defined as:

$$D_F^{\alpha} f(t) = \begin{cases} F\text{-}\lim_{y \to t} \frac{f(y)-f(t)}{S_F^{\alpha}(y)-S_F^{\alpha}(t)}, & t \in F \cap [a,b] \\ 0, & otherwise \end{cases} \tag{1}$$

where $S_F^{\alpha}(t)$ is the Staircase function of order α defined for the set F. Whenever f has a fractal derivative at every point $t \in [a,b]$ we say that f is F^{α}-derivable on $[a,b]$.

Proposition 2.1. *Let $f : [a,b] \to \mathbb{R}$ and $g : [a,b] \to \mathbb{R}$ be two real functions that are F^{α}-derivable on each point $t \in [a,b]$. Then, we have:*

$$D_F^{\alpha}(f+g)(t) = D_F^{\alpha} f(t) + D_F^{\alpha} g(t),$$

$$D_F^{\alpha}(fg)(t) = f(t) D_F^{\alpha} g(t) + g(t) D_F^{\alpha} f(t),$$

$$D_F^{\alpha}\left(\frac{f}{g}\right)(t) = \frac{g(t) D_F^{\alpha} f(t) - f(t) D_F^{\alpha} g(t)}{g^2(t)}.$$

Definition 6. The characteristic function $\chi_F : [a,b] \to \mathbb{R}$ of the fractal set F is defined by

$$\chi_F(t) = \begin{cases} 1, & t \in F \cap [a,b]; \\ 0, & otherwise. \end{cases} \tag{2}$$

Remark 2.3. Let us observe that:

- $\chi_F \in C(F \cap [a,b])$,
- $D_F^{\alpha} S_F^{\alpha}(t) = \chi_F(t), \quad \forall t \in [a,b]$

Definition 7. Let $f : [a,b] \to \mathbb{R}$. If f is F^{α}-derivable at every point $t \in [a,b]$, then the F^{α}-derivative function $D_F^{\alpha} f : [a,b] \to \mathbb{R}$ is well defined.

1. If $D_F^{\alpha} f(t)$ is F-continuous therefore we say that f belongs to the space $C^1(F \cap [a,b])$.

2. If $D_F^\alpha f(t)$ is F^α-derivable at $t \in F$, we say that f has a 2α-fractal derivative at t, denoted by $D_F^{2\alpha} f(t) := D_F^\alpha(D_F^\alpha f(t))$.

Remark 2.4. It is trivial to observe that:

$$D_F^{2\alpha} S_F^\alpha(t) = D_F^\alpha(D_F^\alpha S_F^\alpha(t)) = D_F^\alpha \chi_F(t) = 0, \quad \forall t \in [a,b]$$

Definition 8. Let $f : [a,b] \to \mathbb{R}$ and let $\Psi : [a,b] \to \mathbb{R}$ be two real functions. We say that Ψ is a fractal-primitive of f, if Ψ is F^α-derivable on $[a,b]$ and we have that

$$D_F^\alpha(\Psi(t)) = \begin{cases} f(t), & t \in F \cap [a,b]; \\ 0, & otherwise. \end{cases} \tag{3}$$

Example 2.1. By Remark 2.3 it follows that the staircase function associated with the fractal set F of order α is a fractal-primitive of the characteristic function χ_F.

Proposition 2.2. *Let $f : [a,b] \to \mathbb{R}$. If $f(t)$ admits a fractal-primitive $\Psi(t)$ on every point $t \in F \cap [a,b]$, then for every constant $S_F^\alpha(c) \in \mathbb{R}$, the function $\Phi(t) = \Psi(t) + S_F^\alpha(c)$ is a fractal-primitive of $f(t)$.*

The proof is straightforward.

Definition 9. Let $f : [a,b] \to \mathbb{R}$ and let $t \in [a,b]$. The set of change of f, symbolized as $Sch(f)$, is the collection of all such points t where the behavior of the function is locally non-constant. Formally:

$$Sch(f) = \{t \in [a,b] : \forall \delta > 0, \exists y_1, y_2 \in (t-\delta, t+\delta) \cap [a,b], \; such that \; f(y_1) \neq f(y_2)\}$$

Example 2.2. Let $S_F^\alpha(c) \in \mathbb{R}$ and let $f_1(t) = S_F^\alpha(c)$, therefore $\mathrm{Sch}(f_1) = \emptyset$. Let $f_2(t) = t$, for every $t \in [a,b]$, therefore $\mathrm{Sch}(f_2) = [a,b]$.

Proposition 2.3. *Let $\Psi : [a,b] \to \mathbb{R}$ and $\Phi : [a,b] \to \mathbb{R}$ be two fractal-primitives of $f : [a,b] \to \mathbb{R}$. If $Sch(\Psi - \Phi) \subset F \cap [a,b]$, therefore there exists a constant $S_F^\alpha(c) \in \mathbb{R}$ such that $\Psi(t) = \Phi(t) + S_F^\alpha(c)$ for every $t \in F \cap [a,b]$.*

Proof. Define $H(t) = \Psi(t) - \Phi(t)$, for all $t \in F \cap [a,b]$. By hypothesis we have $D_F^\alpha(H(t)) = D_F^\alpha \Psi(t) - D_F^\alpha \Phi(t) = f(t) - f(t) = 0$, for all $t \in F \cap [a,b]$. The conclusion then follows by applying the Corollary 52 in [20] to the function H. □

Definition 10. Let $f : [a,b] \to \mathbb{R}$. The set of all fractal-primitives, of f on $F \cap [a,b]$ is called the indefinite F^α−integral and is denoted by the symbol

$$\int f(t) d_F^\alpha t$$

Example 2.3. By Remark 2.3 it follows

$$\int \chi_F(t) d_F^\alpha t = S_F^\alpha(t) + S_F^\alpha(c)$$

3. Solving equations of the form: $D_F^\alpha \; y(t) = g(\phi(y,t))$

In this section, we address the class of homogeneous nonlinear fractal differential equations defined by:

$$D_F^\alpha y(t) = g(\phi(y,t)), \quad \text{with } t \in F \cap [a,b]$$

where $\phi(y,t)$ is an assigned function. We establish that a carefully selected change of variables effectively reduces this complex nonlinear problem into a more tractable linear fractal differential equation with separable variables, thereby facilitating its study and analytical solution.

3.1. First case: $\phi(y,t) = \frac{y(t)}{S_F^\alpha(t)}$

The fractal differential equation we aim to solve has the form:

$$D_F^\alpha y(t) = g\left(\frac{y(t)}{S_F^\alpha(t)}\right), \tag{4}$$

To solve this equation, we make the substitution

$$y(t) = S_F^\alpha(t) z(t). \tag{5}$$

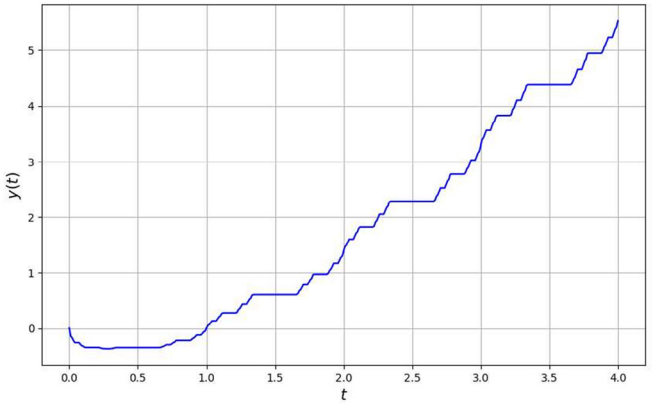

Fig. 2. Plot of Eq. (7).

Applying Proposition 2.1 to both sides of Eq. (5), we have:

$$D_F^\alpha y(t) = z(t)\chi_F(t) + S_F^\alpha(t) D_F^\alpha z(t).$$

Substituting this into the original equation, we obtain the following fractal differential equation:

$$S_F^\alpha(t)\, D_F^\alpha z(t) + \chi_F(t) z(t) = g(z(t)),$$

which can be solved by the method of separation of variables described in [23].

Example 3.1. Consider the fractal differential equation on the ternary Cantor set $C \subset [0,1]$ given by:

$$D_C^\alpha y(t) = 1 + \frac{y(t)}{S_C^\alpha(t)}. \tag{6}$$

By employing the substitution $y(t) = S_C^\alpha(t) z(t)$ and solving the resulting separable equation (see Appendix A.1 for the detailed derivation), we obtain the exact solution:

$$y(t) = S_C^\alpha(t) \ln\left(S_C^\alpha(c') S_C^\alpha(t)\right), \tag{7}$$

where $S_C^\alpha(c') = \pm \exp(S_C^\alpha(c))$.

Note that in Fig. 2, we depict the graphical representation of the solution to Eq. (6).

3.2. Second case: $\phi(y,t) = aS_F^\alpha(t) + by(t)$ with a and b two non-zero real numbers.

Let us consider a fractal differential equation of the type

$$D_F^\alpha y(t) = g(aS_F^\alpha(t) + by(t)),$$

where g is an F-continuous function and a, b are two non-zero real constants. This equation can be reduced to a fractal differential equation with separable variables by the following substitution:

$$z = aS_F^\alpha(t) + by(t).$$

In fact, since $D_F^\alpha z(t) = a\chi_F(t) + bD_F^\alpha y(t)$, we obtain the equivalent fractal differential equation in the unknown variable z:

$$D_F^\alpha z(t) = a\chi_F(t) + bg(z(t)),$$

which can be solved easily using the separation of variables method (see [23]).

Example 3.2. Let us consider the fractal differential equation on the Cantor set C given by:

$$D_C^\alpha y(t) = \left(S_C^\alpha(t) + y(t)\right)^2. \tag{8}$$

It is easy to observe that here the function g is defined by:

$$g(t) = \left(S_C^\alpha(t) + y(t)\right)^2.$$

Now, by setting $z(t) = S_C^\alpha(t) + y(t)$, and applying the C^α-derivative to both sides, we obtain:

$$D_C^\alpha z(t) = \chi_C(t) + D_C^\alpha y(t),$$

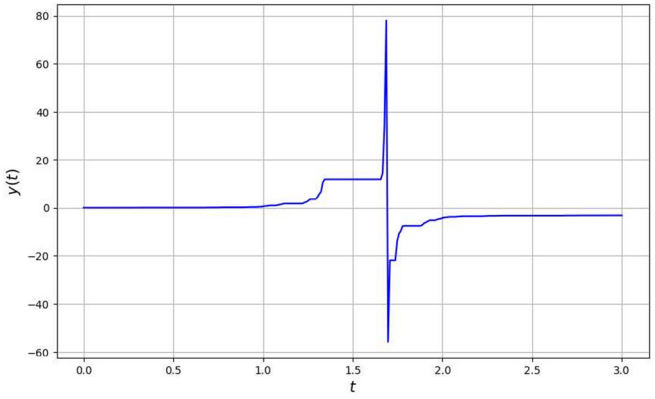

Fig. 3. Plot of Eq. (10).

Therefore,

$$D_C^\alpha z(t) = \chi_C(t) + \left(S_C^\alpha(t) + y(t)\right)^2 = \chi_C(t) + z^2(t).$$

That is,

$$D_C^\alpha z(t) = \chi_C(t) + z^2(t). \tag{9}$$

So, solving it by the separation of variables, we obtain:

$$\arctan z(t) = \int \frac{1}{\chi_C(t) + z^2}\, d_C^\alpha z = \int \chi_C(t) d_C^\alpha t = S_C^\alpha(t) + S_C^\alpha(c),$$

where $S_C^\alpha(c)$ is an arbitrary constant. Thus, solving for $y(t)$, we obtain the exact solution:

$$y(t) = \tan\left(S_C^\alpha(t) + S_C^\alpha(c)\right) - S_C^\alpha(t). \tag{10}$$

Note that in Fig. 3, we depict the graphical representation of the solution of Eq. (8).

4. Solving Riccati-type fractal differential equations

In this section, we provide a comprehensive analysis of a prominent class of nonlinear fractal differential equations: the Riccati-type fractal differential equations (RFDEs). Specifically, we examine equations of the form:

$$D_F^\alpha y(t) = a(t)y(t) + b(t)y^2(t) + c(t), \quad \forall t \in F \cap [a, b], \tag{11}$$

where $a(t)$, $b(t)$, and $c(t)$ are F-continuous functions.

Due to the inherent complexity of the quadratic non-linear term, finding a universal general solution for the RFDE is a challenging task. To thoroughly address this problem and provide a clear methodological pathway, the present section is structurally divided into three parts. First, in Section 4.1, we introduce several analytical strategies (formulated through specific propositions) aimed at deriving exact solutions under appropriate algebraic conditions. Subsequently, in Section 4.2, we critically discuss the operational limitations and computational constraints of these analytical reductions. Finally, in Section 4.3, we present a rigorous empirical numerical validation to quantitatively confirm our theoretical findings and assess the stability of the solutions on singular fractal supports.

4.1. Analytical methods for exact solutions

First of all, let us observe that if $c(t) \equiv 0$ for all $t \in F \cap [a, b]$, then Eq. (11) reduces to the fractal Bernoulli differential equation

$$D_F^\alpha y(t) = a(t)y(t) + b(t)y^2(t),$$

which has already been studied in [23]. Furthermore, if $b(t) \equiv 0$ for all $t \in F \cap [a, b]$, then Eq. (11) becomes the linear fractal differential equation

$$D_F^\alpha y(t) = a(t)y(t) + c(t), \quad t \in F \cap [a, b],$$

which has also been investigated in [23]. For this reason, from now on we will consider Eq. (11) with both coefficients $c(t)$ and $b(t)$ different from zero.

Let us start by describing some solution techniques for the RFDE that are based on the knowledge of a particular solution (see Fig. 4).

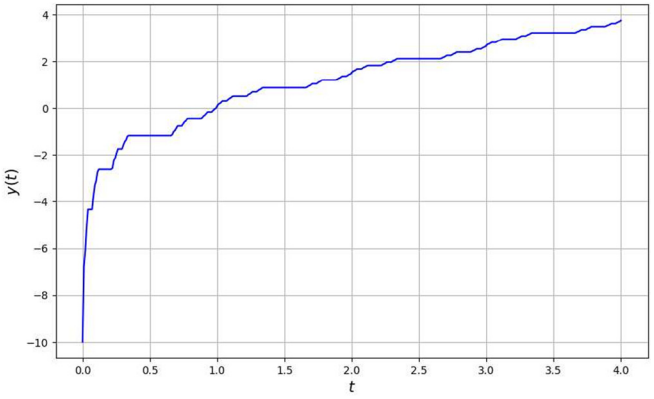

Fig. 4. Plot of Eq. (18).

Proposition 4.1. *Each solution of equation the RFDE (Eq. (11)) has the following form*

$$y(t) = u(t) + v(t), \tag{12}$$

where $u(t)$ is a particular solution of Eq. (11) while $v(t)$ is an exact solution of the following Bernoulli-type fractal differential equation:

$$D_F^\alpha v(t) = (a(t) + 2b(t)u(t))\, v(t) + b(t)v^2(t). \tag{13}$$

Proof. Let $u(t)$ be a particular solution of Eq. (11), and let $v(t)$ be an exact solution of Eq. (13). We aim to show that

$$y(t) = u(t) + v(t) \tag{14}$$

is a general solution of Eq. (11). Therefore, applying Proposition 2.1 to both members of Eq. (14) and requiring that the function $u(t) + v(t)$ satisfies Eq. (11), we get:

$$\begin{aligned} D_F^\alpha y(t) &= D_F^\alpha u(t) + D_F^\alpha v(t) \\ &= a(t)(u(t) + v(t)) + b(t)(u(t) + v(t))^2 + c(t) \\ &= \left[a(t)u(t) + b(t)u^2(t) + c(t)\right] + a(t)v(t) + 2b(t)u(t)v(t) + b(t)v^2(t). \end{aligned} \tag{15}$$

Since $u(t)$ satisfies Eq. (11) and $v(t)$ satisfies Eq. (13), the equation holds true. Hence, $y(t) = u(t) + v(t)$ is indeed an exact solution of Eq. (11). □

Unfortunately, there is no general algorithm for finding the particular solution $u(t)$, as it depends on the specific forms of the functions $a(t)$, $b(t)$, and $c(t)$. In the following, we present an example to illustrate the method.

Example 4.1. Consider the following RFDE on the Cantor set C:

$$D_C^\alpha y(t) + 2S_C^\alpha(t)y(t) = \chi_C(t) + \left(S_C^\alpha(t)\right)^2 + y^2(t). \tag{16}$$

Here the functions $a(t)$, $b(t)$, and $c(t)$ are respectively: $a(t) = 2S_C^\alpha(t)$, $b(t) = 1$ and $c(t) = \chi_C(t) + \left(S_C^\alpha(t)\right)^2$. Moreover, $u(t) = S_C^\alpha(t)$ is a particular solution of Eq. (16). Indeed, since $D_C^\alpha S_C^\alpha(t) = \chi_C(t)$ (see Remark 2.3), it is trivial to verify that

$$D_C^\alpha u(t) = -2S_C^\alpha(t)u(t) + u^2(t) + \chi_C(t) + \left(S_C^\alpha(t)\right)^2. \tag{17}$$

To obtain the general solution of Eq. (16), we apply Proposition 4.1. The detailed steps are provided in Appendix A.2. The general solution is given by:

$$y(t) = S_C^\alpha(t) - \frac{1}{S_C^\alpha(t) + S_C^\alpha(c)}. \tag{18}$$

Proposition 4.2. *Each solution of equation the RFDE (Eq. (11)) has the following form*

$$y(t) = u(t) + \frac{1}{v(t)}, \quad \forall t \in F, \tag{19}$$

where $u(t)$ is a particular solution of Eq. (11) while $v(t)$ is an exact solution of the following linear fractal differential equation:

$$D_F^\alpha v(t) = -\left(a(t) + 2b(t)u(t)\right) v(t) - b(t). \tag{20}$$

Proof. Let $u(t)$ be a particular solution of the RFDE (Eq. (11)) and let $v(t)$ be an exact solution of the linear fractal differential equation given by Eq. (20). We aim to show that

$$y(t) = u(t) + \frac{1}{v(t)} \tag{21}$$

is a solution of the RFDE. By applying Proposition 2.1 to calculate the F^α-derivative of both sides of Eq. (21), we obtain:

$$D_F^\alpha y(t) = D_F^\alpha u(t) - \frac{D_F^\alpha v(t)}{v^2(t)}. \tag{22}$$

Substituting the expression for $D_F^\alpha v(t)$ from Eq. (20) into Eq. (22), we have:

$$\begin{aligned} D_F^\alpha y(t) &= D_F^\alpha u(t) - \frac{-\left(a(t) + 2b(t)u(t)\right) v(t) - b(t)}{v^2(t)} \\ &= D_F^\alpha u(t) + \frac{a(t) + 2b(t)u(t)}{v(t)} + \frac{b(t)}{v^2(t)}. \end{aligned}$$

Since $u(t)$ is a particular solution of Eq. (11), it satisfies $D_F^\alpha u(t) = a(t)u(t) + b(t)u^2(t) + c(t)$. Substituting this into the equation above, we get:

$$\begin{aligned} D_F^\alpha y(t) &= \left[a(t)u(t) + b(t)u^2(t) + c(t)\right] + \frac{a(t)}{v(t)} + \frac{2b(t)u(t)}{v(t)} + \frac{b(t)}{v^2(t)} \\ &= a(t)\left(u(t) + \frac{1}{v(t)}\right) + b(t)\left(u^2(t) + \frac{2u(t)}{v(t)} + \frac{1}{v^2(t)}\right) + c(t) \\ &= a(t)\left(u(t) + \frac{1}{v(t)}\right) + b(t)\left(u(t) + \frac{1}{v(t)}\right)^2 + c(t). \end{aligned}$$

By observing the structure of $y(t)$ in Eq. (21), we can rewrite the last expression as:

$$D_F^\alpha y(t) = a(t)y(t) + b(t)y^2(t) + c(t).$$

Thus, $y(t) = u(t) + 1/v(t)$ is indeed an exact solution of the RFDE. □

Remark 4.1. The method described in Proposition 4.2 offers a distinct methodological advantage compared to the one presented in Proposition 4.1. While Proposition 4.1 transforms the RFDE into a Bernoulli-type equation (which is still non-linear and requires further substitution), Proposition 4.2 reduces the problem *directly* to a linear fractal differential equation. This direct linearization significantly streamlines the analytical resolution. We now demonstrate how Proposition 4.2 allows us to solve the RFDE proposed in Example 4.1 more efficiently. Indeed, the linear differential equation associated with the RFDE is:

$$D_F^\alpha v(t) = -1.$$

Therefore the exact solution of Eq. (16) is immediately obtained as:

$$y(t) = S_F^\alpha(t) + \frac{1}{S_F^\alpha(c) - S_F^\alpha(t)}. \tag{23}$$

where $S_F^\alpha(c)$ is a constant.

To better describe the method proposed by Proposition 4.2, let us examine the following example:

Example 4.2. Let

$$D_F^\alpha y(t) = \frac{1}{S_F^\alpha(t)} y(t) + y^2(t) - 4(S_F^\alpha(t))^2 \tag{24}$$

be a RFDE defined on a fractal subset of the real line $F \subset [0, 1]$.

It is trivial to observe that $u(t) = 2S_F^\alpha(t)$ is a particular solution of Eq. (24). Let us show that an exact solution of the proposed RFDE is of the form:

$$y(t) = u(t) + \frac{1}{v(t)} = 2S_F^\alpha(t) + \frac{1}{v(t)}, \quad \forall t \in F, \tag{25}$$

where the function $v(t)$ is to be determinated. Let us F^α-derive both members of the Eq. (25):

$$D_F^\alpha y(t) = 2\,\chi_F(t) - \frac{D_F^\alpha v(t)}{v^2(t)}$$

and impose that Eq. (25) verifies Eq. (24), so we obtain:

$$2\,\chi_F(t) - \frac{D_F^\alpha v(t)}{v^2(t)} = \frac{1}{S_F^\alpha(t)}\left(2S_F^\alpha(t) + \frac{1}{v(t)}\right) + \left(2S_F^\alpha(t) + \frac{1}{v(t)}\right)^2 - 4(S_F^\alpha(t))^2. \tag{26}$$

Now, solving Eq. (26) with respect to $v(t)$, we get:

$$D_F^\alpha v(t) = -\left(4S_F^\alpha(t) + \frac{1}{S_F^\alpha(t)}\right) v(t) - 1. \tag{27}$$

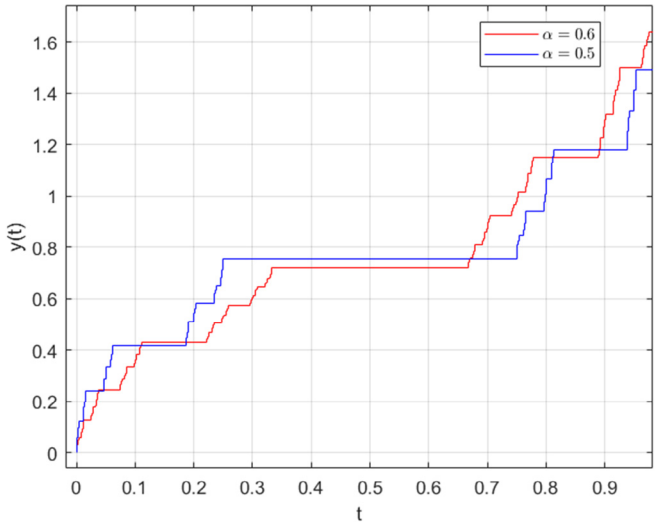

Fig. 5. Plot of Eq. (29) for different fractal subsets of the real line.

Finally, following methods in [23] we have that the exact solution of Eq. (27) is

$$v(t) = \frac{e^{(-S_F^\alpha(t))^2}}{S_F^\alpha(t)}\left(-\frac{e^{(S_F^\alpha(t))^2}}{S_F^\alpha(t)} + S_F^\alpha(c)\right), \tag{28}$$

where $S_F^\alpha(c)$ is a constant.

Therefore the exact solution of Eq. (24) is:

$$y(t) = 2S_F^\alpha(t) + \frac{1}{\frac{e^{(-S_F^\alpha(t))^2}}{S_F^\alpha(t)}\left(-\frac{e^{(S_F^\alpha(t))^2}}{S_F^\alpha(t)} + S_F^\alpha(c)\right)}, \quad \forall t \in F. \tag{29}$$

In Fig. 5, we show the effect of the support of the function on the solution with dimensions $\alpha = 0.5$ and $\alpha = 0.6$.

Proposition 4.3. *Let $b : F \cap [a,b] \to \mathbb{R}$ be a positive function such that $b \in C^1(F \cap [a,b])$. Let $z(t)$ be a solution of the following second-order fractal differential equation:*

$$D_F^{2\alpha} z(t) = \left(\frac{D_F^\alpha b(t)}{b(t)} + a(t)\right) D_F^\alpha z(t) - b(t)c(t)z(t), \quad \forall t \in F \cap [a,b], \tag{30}$$

Then the RFDE (Eq. (11)) has an exact solution of the form

$$y(t) = -\frac{D_F^\alpha z(t)}{b(t)z(t)}, \qquad \forall t \in F \cap [a,b]. \tag{31}$$

Proof. Let us suppose that $z(t)$ is a solution of Eq. (30) and let us show that

$$y(t) = -\frac{D_F^\alpha z(t)}{b(t)z(t)}, \tag{32}$$

is a solution of Eq. (11).

To do this, by taking the F^α-derivative of both sides of the previous equation:

$$\begin{aligned} D_F^\alpha y(t) &= D_F^\alpha\left(-\frac{D_F^\alpha z(t)}{b(t)z(t)}\right) \\ &= \frac{-b(t)z(t)D_F^{2\alpha} z(t) + z(t)D_F^\alpha z(t)D_F^\alpha b(t) + b(t)(D_F^\alpha z(t))^2}{b^2(t)z^2(t)} \end{aligned} \tag{33}$$

and impose that Eq (33) satisfies Eq. (11).

Therefore, we have:

$$\frac{-b(t)z(t)D_F^{2\alpha} z(t) + z(t)D_F^\alpha z(t)D_F^\alpha b(t) + b(t)(D_F^\alpha z(t))^2}{b^2(t)z^2(t)} \tag{34}$$

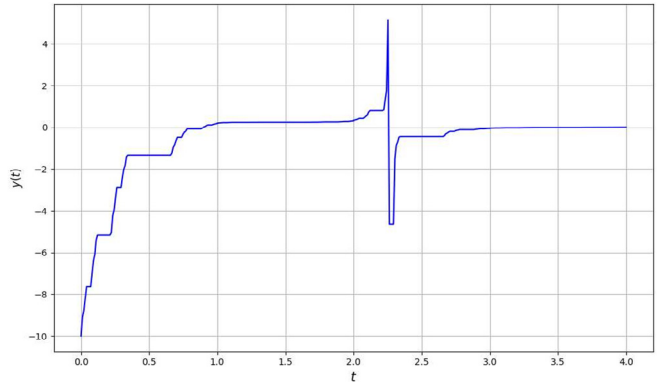

Fig. 6. Plot of Eq. (39), where $S_C^\alpha(t)$ is the integral staircase function based on the middle-third Cantor set.

$$= -\frac{a(t)D_F^\alpha z}{b(t)z(t)} + b(t)\left(\frac{D_F^\alpha z(t)}{b(t)z(t)}\right)^2 + c(t). \tag{35}$$

Now, multiplying both sides by $b(t)z(t)$ and simplifying the equation, we obtain:

$$-D_F^{2\alpha} z(t) + \frac{D_F^\alpha b(t)}{b(t)} D_F^\alpha z(t) = -a(t)D_F^\alpha z(t) + b(t)c(t)z(t). \tag{36}$$

Finally, rearranging terms gives the required second-order fractal differential equation:

$$D_F^{2\alpha} z(t) = \left(\frac{D_F^\alpha b(t)}{b(t)} + a(t)\right) D_F^\alpha z(t) - b(t)c(t)z(t), \quad \forall t \in F \cap [a,b]. \quad \square \tag{37}$$

Example 4.3. Let C be the classical Cantor set and let

$$D_C^\alpha y(t) = -\frac{3}{S_C^\alpha(t)} y(t) + (S_C^\alpha(t))^3 y^2 + \frac{1}{(S_C^\alpha(t))^3}, \tag{38}$$

be the RFDE defined on each point of C. It is trivial to notice that $b(t) = \left(S_C^\alpha(t)\right)^3 \in C^1(C)$ on each point of C, therefore, to solve Eq. (38), we can apply Proposition 4.3. As detailed in Appendix A.3, applying Proposition 4.3 allows us to derive the exact general solution:

$$y(t) = \frac{\sin(S_C^\alpha(t)) - c\cos(S_C^\alpha(t))}{(S_C^\alpha(t))^3(\cos(S_C^\alpha(t)) + S_C^\alpha(c)\sin(S_C^\alpha(t)))}. \tag{39}$$

where $S_C^\alpha(c)$ is a constant.

Note that Fig. 6 shows the graph of Eq. (39) with the constant $S_C^\alpha(c) = 1$.

4.2. Limitations of the proposed method

While the analytical methods presented in this section provide exact solutions for Riccati-type fractal differential equations, it is important to acknowledge their limitations. Specifically, the strategies developed here (see Propositions 4.1 and 4.2) rely fundamentally on the knowledge of a particular solution $u(t)$. The transformation of the non-linear RFDE into a solvable linear or Bernoulli-type fractal equation is contingent upon the existence and identification of this specific solution. In many practical scenarios, finding a particular solution $u(t)$ is non-trivial and often requires heuristic methods, symmetry analysis, or inspection of the coefficients $a(t)$, $b(t)$, and $c(t)$. If a particular solution cannot be identified analytically, these reduction methods cannot be applied directly.

To circumvent the need for a priori knowledge of $u(t)$, Proposition 4.3 offers an alternative approach by transforming the first-order non-linear RFDE into a second-order linear fractal differential equation. However, this method introduces its own inherent challenge: solving a second-order linear FDE with variable coefficients is generally not straightforward and can be mathematically as demanding as solving the original non-linear Riccati equation.

A systematic summary of these analytical strategies and their respective operational constraints is provided in Table 1.

In such cases where analytical reduction is unfeasible,one must resort to numerical approximation techniques, such as the generalized Fractal Euler Method extensively discussed in the next section. Consequently, while the proposed framework offers a rigorous pathway to exact solutions where possible, it does not constitute a universal algorithm for all Riccati-type fractal differential equations without the support of high-resolution numerical scheme.

Table 1
Summary of analytical methods for Riccati-type FDEs and their operational limitations.

Method strategy	Transformation target	Main limitation
Bernoulli Reduction (Proposition 4.1)	Reduces RFDE to a Bernoulli-type fractal equation.	Requires the knowledge of a particular solution $u(t)$. No general algorithm exists to find it.
Linear Reduction (Proposition 4.2)	Reduces RFDE to a first-order Linear fractal equation.	Also requires a particular solution $u(t)$. If $u(t)$ is unknown, the method cannot be started.
Second-Order Transformation (Proposition 4.3)	Transforms RFDE into a second-order linear FDE.	Does not require $u(t)$, but solving the resulting second-order linear equation can be as complex as the original problem.

4.3. Numerical validation and empirical error analysis

Having derived exact analytical solutions for Riccati-type fractal differential equations, we now verify their consistency through numerical simulations. We focus on Example 4.1 as a fundamental test case to demonstrate how the analytical results remain robust under discrete iterative schemes on singular supports like the Cantor set. This reliable approach can be easily extended to other scenarios, following the general algorithmic framework outlined at the end of this section.

The simulation employs a generalized Fractal Euler Method, whose implementation follows the framework established by A.K.G., A.I. Zayed, and R. Myrzakulov [29] for non-linear dynamics on fractal supports. The computational parameters are summarized below:

Fractal support	Standard ternary Cantor set $C \subset [0,1]$
Fractal Dimension	$\alpha = \ln 2 / \ln 3 \approx 0.6309$
Riccati-type FDE	$D_C^\alpha y(t) = -2S_C^\alpha(t)y(t) + y^2(t) + \chi_C(t) + (S_C^\alpha(t))^2$
Initial Condition	$y(0) = -10 \implies S_C^\alpha(c) = 0.1$
Exact Solution	$y(t) = S_C^\alpha(t) - [S_C^\alpha(t) + S_C^\alpha(c)]^{-1}$

To derive the numerical scheme, we first express the fractal differential equation at a discrete point $t = t_n$:

$$D_C^\alpha y(t)|_{t=t_n} = k(t_n, y(t_n)) \tag{40}$$

where the right-hand side function for our specific Riccati-type equation is defined as $k(t,y) = -2S_C^\alpha(t)y(t) + y^2(t) + \chi_C(t) + (S_C^\alpha(t))^2$. The related fractal forward difference quotient is then used to approximate the fractal derivative. This relates the variation of the unknown function to the step size of the staircase function $S_C^\alpha(t)$, yielding:

$$\frac{y(t_{n+1}) - y(t_n)}{S_C^\alpha(t_{n+1}) - S_C^\alpha(t_n)} \cong k(t_n, y(t_n)) \tag{41}$$

Lastly, by solving for the next step and replacing the exact theoretical values with the approximate numerical values y_{n+1} and y_n, we arrive at the general formula for the Fractal Euler Method:

$$y_{n+1} = y_n + k(t_n, y_n)\left(S_C^\alpha(t_{n+1}) - S_C^\alpha(t_n)\right) \tag{42}$$

By substituting our explicit expression for $k(t_n, y_n)$, we implemented the following iterative scheme on the Cantor set support:

$$y_{n+1} = y_n + \left[S_C^\alpha(t_{n+1}) - S_C^\alpha(t_n)\right]\left(-2S_C^\alpha(t_n)y_n + y_n^2 + \chi_C(t_n) + (S_C^\alpha(t_n))^2\right) \tag{43}$$

The comparison between the exact solution and the numerical approximation is depicted in Fig. 7.

Unlike the unstable divergence often encountered in non-linear fractal simulations, the corrected numerical integration (blue dashed line) exhibits excellent agreement with the analytical solution (red continuous line). Both curves accurately capture the characteristic "plateaus", which represent periods of stasis corresponding to the gaps in the fractal support. As established in [29], these flat regions coincide with the complementary intervals of the Cantor set where the staircase function $S_C^\alpha(t)$ remains constant. These results confirm the robustness of the derived formulas and the stability of the Fractal Euler Method for Riccati-type equations when properly adapted to the fractal topology.

To quantitatively ground the visual agreement shown in Fig. 7, we conduct an empirical error analysis. At any given discrete point t_n, the discrepancy between the exact analytical solution $y(t_n)$ and the numerical approximation y_n is quantified by the global error:

$$\mathcal{E}_n = y(t_n) - y_n \tag{44}$$

Based on this definition, we compute two standard metrics to evaluate the overall accuracy over the entire grid: the Maximum Absolute Error, defined as $\max_n |\mathcal{E}_n|$, and the L^2 norm of the error. Table 2 reports these metrics for two different grid resolutions ($N = 1000$ and $N = 10,000$). The results highlight a fundamental aspect of numerical integration on singular spaces. Due to the nonlinear nature of the Riccati equation and the topology of the Cantor set, a coarse grid ($N = 1000$) fails to accurately capture the

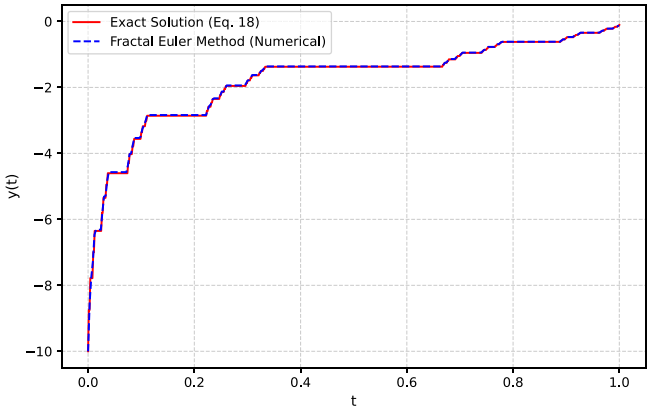

Fig. 7. Numerical validation of the Riccati-type fractal differential equation on the Cantor set. Comparison between the exact analytical solution and the Fractal Euler Method.

Table 2
Empirical error analysis for the generalized Fractal Euler Method applied to the RFDE on the Cantor set.

Grid steps (N)	$\max_n \lvert\mathcal{E}_n\rvert$	L^2 norm error	Observation
1000	8.568×10^3	2.743×10^2	Unstable (misses fractal gaps)
10,000	1.334×10^0	4.314×10^{-1}	Stable convergence

Table 3
Pseudocode of the generalized Fractal Euler Method.

Input: Fractal subset F and its dimension α, integration interval $[t_0, t_N]$, number of steps N, initial condition $y_0 = y(t_0)$, right-hand side function $k(t, y)$, and the Staircase function $S_F^\alpha(t)$.
Output: Arrays T and Y containing the discrete time steps and approximate solution.

$h \leftarrow (t_N - t_0)/N$ *(Define uniform classical time step)*
$T[0] \leftarrow t_0$, $Y[0] \leftarrow y_0$ *(Initialize arrays)*
for $n = 0$ **to** $N - 1$ **do**
  $t_{n+1} \leftarrow T[n] + h$ *(Compute next continuous time point)*
  $\Delta S \leftarrow S_F^\alpha(t_{n+1}) - S_F^\alpha(T[n])$ *(Compute fractal step size h_F^α)*
  $k_n \leftarrow k(T[n], Y[n])$ *(Evaluate right-hand side function)*
  $Y[n+1] \leftarrow Y[n] + \Delta S \cdot k_n$ *(Fractal Euler update)*
  $T[n+1] \leftarrow t_{n+1}$ *(Store time step)*
end for
return T, Y

flat plateaus of the staircase function $S_C^\alpha(t)$. However, refining the grid to $N = 10,000$ effectively stabilizes the solution, bounding the maximum absolute error to roughly 1.33 and dropping the L^2 error to 0.43. This quantitative validation firmly confirms the correctness of our exact analytical solutions. At the same time, it emphasizes a practical computational limitation: discrete simulations on fractals supports intrinsically require high-resolution grids to properly account for the non-differentiable gaps of the structure.

Remark 4.2. In light of the preceding analysis, we observe that to complete the study of the numerical simulation and, most importantly, to adapt it to a generic RFDE, it is necessary to detail the computational implementation. To ensure the full reproducibility of these findings, Table 3 outlines the step-by-step algorithmic logic of the generalized Fractal Euler Method used in our study. By defining the specific fractal support F (the Cantor set C or the generalized Cantor set $C(\lambda)$), the corresponding staircase function $S_F^\alpha(t)$ and the right-hand side function $k(t, y)$ as inputs, the algorithm iteratively computes the exact numerical approximation based on the fractal difference quotient. The integration step is uniquely driven by the variation of the staircase function, denoted by ΔS, naturally bypassing the non-differentiable flat plateaus of the fractal subset F.

Furthermore, our choice of the Fractal Euler Method aligns with recent findings [29]. Due to the fragmented nature of fractal solutions, this simple scheme surprisingly outperforms higher-order methods (such as Heun or Runge–Kutta) in accuracy, making it a highly efficient tool for complex systems.

5. Fractal Riccati formulation of the Schrödinger equation

Having established both analytical strategies and their numerical validation for Riccati-type fractal differential equations (RFDEs), we now transition from pure mathematics to applied modeling. Indeed, these equations naturally emerge when describing complex systems governed by non-integer dimensions.

In this section we show how the RFDE intervenes in the formulation of the Schrödinger equation on fractal domains. This connection explicitly demonstrates how the mathematical framework of Riccati-type FDEs relates to fundamental physics, thereby highlighting the potential applications of our theory in quantum mechanics and mathematical physics. It shows that the solution techniques developed for RFDEs can be directly employed to solve Schrödinger equations on fractal sets, emphasizing the interdisciplinary value of the proposed method.

The time-independent α-dimensional Schrödinger fractal equation [30] on an α-perfect fractal set F is given by

$$-\frac{\hbar^2}{2m}D_F^{2\alpha}\psi(t)+V(t)\psi(t)=E\psi(t),\quad \forall t\in F, \tag{45}$$

where $V(t)$ is the potential, $\psi(t)$ the wavefunction, and E the energy eigenvalue. An efficient method for its study is the *factorization approach* [31], in which the Hamiltonian is written as a product of first α-order operators:

$$A=D_F^{\alpha}+W(t),\qquad A^{\dagger}=-D_F^{\alpha}+W(t), \tag{46}$$

where D_F^{α} is the F^{α}-derivative operator and $W(t)$ is the *superpotential* [32]. The Hamiltonian becomes

$$H=A^{\dagger}A=-D_F^{2\alpha}+W(t)^2-D_F^{\alpha}W(t). \tag{47}$$

Thus the potential is related to $W(t)$ through the RFDE:

$$V(t)=W(t)^2-D_F^{\alpha}W(t),\quad \forall t\in F. \tag{48}$$

The superpotential itself is connected with the ground-state wavefunction $\psi_0(t)$ via

$$W(t)=-D_F^{\alpha}\ln\psi_0(t). \tag{49}$$

This provides a direct link between the RFDE and the quantum system under consideration.

To explicitly clarify this connection and demonstrate that our previous analysis is far from being a purely theoretical exercise, it is highly instructive to map the terms of the generalized RFDE to the physical parameters of the quantum system.

Recall the generalized RFDE analyzed in Section 4, given by Eq. (11):

$$D_F^{\alpha}y(t)=a(t)y(t)+b(t)y^2(t)+c(t). \tag{50}$$

In the context of Supersymmetric Quantum Mechanics (SUSY QM) and the factorization of the fractal Schrödinger equation, this Riccati structure emerges naturally. The general unknown function $y(t)$ corresponds directly to the *superpotential*, denoted as $W(t)$. Consequently, the abstract mathematical coefficients map to the physical parameters as follows:

- $a(t)=0$: The linear term is absent in the standard factorization of the Schrödinger equation.
- $b(t)=\pm1$: This constant coefficient defines the quadratic nature of the superpotential (the sign depends on the specific forward or backward factorization operator applied).
- $c(t)=E-V(t)$ (or $V(t)-E$): The known term $c(t)$ is entirely determined by the physics of the system, representing the difference between the energy level E (typically the ground state energy) and the fractal potential $V(t)$ acting on the particle.

Therefore, applying the analytical reductions and the numerical methods developed in Section 4 for this specific set of coefficients ($a=0$, $b=\pm1$, $c=E-V$) is mathematically equivalent to determining the exact superpotential $W(t)$. Once $W(t)$ is analytically or numerically found, the corresponding fractal Schrödinger equation is exactly solvable.

Example 5.1. Let $F\subset\mathbb{R}$ be an α-perfect fractal set. Let us consider the fractal harmonic oscillator potential for the Harmonic Oscillator

$$V(x)=\tfrac{1}{2}m\omega^2S_F^{\alpha}(x)^2,\quad \forall x\in F. \tag{51}$$

Note that here $S_F^{\alpha}(x)$ denotes the α-dimensional fractal coordinate [30]. The normalized ground-state wavefunction [31] is

$$\psi_0(x)\propto\exp\left(-\tfrac{m\omega}{2\hbar}S_F^{\alpha}(x)^2\right). \tag{52}$$

From the logarithmic derivative, the superpotential is

$$W(x)=-D_F^{\alpha}\ln\psi_0(x)=\sqrt{\tfrac{m\omega}{2\hbar}}\,S_F^{\alpha}(x). \tag{53}$$

Substitution into (48) confirms that this $W(x)$ satisfies the RFDE, showing that the fractal harmonic oscillator is exactly solvable by the factorization method [31]. From the perspective of our theoretical framework, the exact analytical methods detailed in Section 4 can be directly applied to determine this exact solution $W(x)$ of the underlying Riccati equation. Furthermore, this system

provides an ideal physical benchmark: should nonlinear perturbations be introduced to the potential $V(x)$ rendering exact solutions unfeasible, the Generalized Fractal Euler Method validated in Section 4 could be seamlessly deployed to numerically integrate the superpotential, ensuring stability across the fractal gaps.

Example 5.2. Let $F \subset \mathbb{R}$ be an α-perfect fractal set. Let us consider the fractal Coulomb potential for the Hydrogen atom:

$$V(r) = -\frac{e^2}{4\pi\epsilon_0}\frac{1}{S_F^\alpha(r)}, \quad \forall r \in F, \quad r > 0. \tag{54}$$

In atomic units ($\hbar = m = e^2/4\pi\epsilon_0 = 1$), the effective radial equation for $u(r) = S_F^\alpha(r)R_{n\ell}(r)$ reads

$$-\tfrac{1}{2}D_F^{2\alpha}u(r) + \left[\frac{\ell(\ell+1)}{2S_F^\alpha(r)^2} - \frac{1}{S_F^\alpha(r)}\right]u(r) = Eu(r). \tag{55}$$

The RFDE for the superpotential $W_\ell(r)$ is

$$W_\ell(r)^2 - D_F^\alpha W_\ell(r) = \frac{\ell(\ell+1)}{S_F^\alpha(r)^2} - \frac{2}{S_F^\alpha(r)} - E_0, \quad \forall r \in F. \tag{56}$$

For the ground state ($n = 1, \ell = 0$), the radial solution is

$$u_{10}(r) \propto \exp(-S_F^\alpha(r)), \tag{57}$$

giving

$$W_0(r) = -D_F^\alpha \ln u_{10}(r). \tag{58}$$

For general ℓ, one finds

$$W_\ell(r) = \frac{\ell+1}{S_F^\alpha(r)} - \frac{1}{\ell+1}, \tag{59}$$

which solves (56). The partner potentials are then

$$V_-(r) = \frac{\ell(\ell+1)}{S_F^\alpha(r)^2} - \frac{2}{S_F^\alpha(r)} - \frac{1}{(\ell+1)^2}, \tag{60}$$

$$V_+(r) = \frac{(\ell+1)(\ell+2)}{S_F^\alpha(r)^2} - \frac{2}{S_F^\alpha(r)} - \frac{1}{(\ell+1)^2}. \tag{61}$$

This demonstrates the *shape invariance* of the Coulomb potential under supersymmetric factorization, with $V_+(r)$ corresponding to the effective potential of angular momentum $\ell+1$. Since Eq. (56) perfectly embodies the general RFDE structure solved in Section 4, the Riccati-type fractal formulation provides more than just a powerful algebraic route to the hydrogen atom spectrum. It also serves as a prime physical candidate for our numerical validation techniques: simulating this equation via the Generalized Fractal Euler Method allows researchers to computationally verify the stability of quantum energy states on highly irregular, non-integer dimensional supports.

6. Conclusion

In this paper, the F^α-calculus was studied and utilized to obtain the exact solutions of various classes of non-linear fractal differential equations. Specifically, we first demonstrated how appropriate changes of variables can reduce complex homogeneous and linear-argument FDEs into tractable equations with separable variables. Subsequently, particular attention was devoted to Riccati-type fractal differential equations (RFDEs).

Beyond the purely theoretical developments, we reinforced our analytical findings through rigorous numerical validation. By implementing a generalized Fractal Euler Method on a singular support like the Cantor set, we demonstrated the stability and computational reliability of the proposed solutions, explicitly showing how the numerical scheme naturally bypasses the non-differentiable gaps inherent to fractal structures.

Furthermore, we extended our mathematical framework to fundamental physics, demonstrating its direct application in quantum mechanics. Specifically, we established that the superpotential in the supersymmetric factorization of the fractal Schrödinger equation is governed precisely by a Riccati-type FDE. Through fundamental physical models – such as the fractal harmonic oscillator and the hydrogen atom – we highlighted how the exact and numerical techniques developed herein provide a powerful tool for analyzing quantum systems in non-integer dimensions.

The examples discussed not only demonstrate the effectiveness of the proposed approach but also open new research directions for the application of F^α-calculus in non-linear differential equations, with potential applications across various scientific and engineering fields, extending the power of fractal methods to more complex non-linear systems. Furthermore, a promising direction for future work is the application of the proposed fractal methods to the stability analysis of neural networks, a field currently investigated primarily through fractional calculus approaches [18,19].

To provide a clear overview of the results obtained, Table 4 summarizes the main categories of fractal differential equations solved in this paper, the specific transformation or substitution methods applied, and the corresponding section references.

Table 4
Summary of solved non-linear fractal differential equations and applied methods.

Equation type	Transformation/Substitution method	Section
Homogeneous FDE $D_F^\alpha y = g(y/S_F^\alpha)$	Substitution $y(t) = S_F^\alpha(t)z(t)$ (Reduces to separable variables)	3
Linear Argument FDE $D_F^\alpha y = g(aS_F^\alpha + by)$	Substitution $z = aS_F^\alpha(t) + by(t)$ (Reduces to separable variables)	3
Riccati-Type (RFDE) $D_F^\alpha y = ay + by^2 + c$	Substitution $y(t) = u(t) + v(t)$ ($u(t)$ is a particular sol.; reduces to Bernoulli FDE)	4
Riccati-Type (RFDE) (Alternative approach)	Substitution $y(t) = u(t) + 1/v(t)$ ($u(t)$ is a particular sol.; reduces to Linear FDE)	4
Riccati-Type (RFDE) (Transformation approach)	Transformation $y(t) = -D_F^\alpha z(t)/(b(t)z(t))$ (Reduces to 2nd order linear FDE)	4

CRediT authorship contribution statement

Donatella Bongiorno: Writing – review & editing, Writing – original draft, Visualization, Methodology, Investigation, Formal analysis, Conceptualization. **Alireza Khalili Golmankhaneh:** Writing – review & editing, Software, Methodology, Investigation, Conceptualization.

Declaration of competing interest

The authors declare that they have no known competing financial interests or personal relationships that could have appeared to influence the work reported in this paper.

Acknowledgments

The authors thank the anonymous referees for their constructive comments, which significantly improved the manuscript.

Appendix. Detailed derivations and calculations

This appendix provides the comprehensive mathematical steps for the analytical solutions discussed in the main text, ensuring the replicability of the results.

A.1. detailed steps for Example 3.1

To solve the equation $D_C^\alpha y(t) = 1 + \frac{y(t)}{S_C^\alpha(t)}$, we utilize the substitution $y(t) = S_C^\alpha(t)z(t)$.

1. Applying Proposition 2.1 to $y(t) = z(t)S_C^\alpha(t)$, we have:

$$D_C^\alpha y(t) = z(t)D_C^\alpha S_C^\alpha(t) + S_C^\alpha(t)D_C^\alpha z(t).$$

2. Utilizing Remark 2.3, we substitute this into the original equation:

$$z(t)\chi_C(t) + S_C^\alpha(t)D_C^\alpha z(t) = \chi_C(t) + z(t).$$

3. Subtracting $z(t)$ from both sides (noting that $\chi_C(t) = 1$ on the support), we obtain:

$$S_C^\alpha(t)D_C^\alpha z(t) = \chi_C(t).$$

4. Solving by separation of variables yields:

$$z(t) = \int \frac{\chi_C(t)}{S_C^\alpha(t)}\, d_C^\alpha t = \ln|S_C^\alpha(t)| + S_C^\alpha(c).$$

5. Multiplying back by $S_C^\alpha(t)$, we arrive at the final solution:

$$y(t) = S_C^\alpha(t)\ln\left(S_C^\alpha(c')S_C^\alpha(t)\right).$$

A.2. Detailed steps for Example 4.1

Given the RFDE $D_C^\alpha y(t) + 2S_C^\alpha(t)y(t) = \chi_C(t) + \left(S_C^\alpha(t)\right)^2 + y^2(t)$:

1. First, we verify the particular solution $u(t) = S_C^\alpha(t)$. Since $D_C^\alpha S_C^\alpha(t) = \chi_C(t)$, it satisfies:
$$D_C^\alpha u(t) = -2S_C^\alpha(t)u(t) + u^2(t) + \chi_C(t) + \left(S_C^\alpha(t)\right)^2.$$
2. Applying Proposition 4.1 with the substitution $y(t) = u(t) + v(t)$, we obtain the following Bernoulli-type differential equation for $v(t)$:
$$D_C^\alpha v(t) = v^2(t).$$
3. Solving for $v(t)$, following the methods in [23]:
$$-\frac{1}{v(t)} = S_C^\alpha(t) + S_C^\alpha(c).$$
4. This gives $v(t) = -\frac{1}{S_C^\alpha(t)+S_C^\alpha(c)}$, leading to the general solution:
$$y(t) = S_C^\alpha(t) - \frac{1}{S_C^\alpha(t) + S_C^\alpha(c)}.$$

A.3. Detailed steps for Example 4.3

For the equation $D_C^\alpha y(t) = -\frac{3}{S_C^\alpha(t)}y(t) + (S_C^\alpha(t))^3 y^2 + \frac{1}{(S_C^\alpha(t))^3}$:

1. We apply Proposition 4.3 with $b(t) = (S_C^\alpha(t))^3$, positing a solution of the form:
$$y(t) = -\frac{D_C^\alpha z(t)}{(S_C^\alpha(t))^3 z(t)}.$$
2. Taking the C^α-derivative of $y(t)$ gives:
$$D_C^\alpha y(t) = \frac{-D_C^{2\alpha} z(t)\left((S_C^\alpha(t))^3 z(t)\right) + D_C^\alpha z(t)\left(3z(t)(S_C^\alpha(t))^2 + (S_C^\alpha(t))^3 D_C^\alpha z(t)\right)}{(S_C^\alpha(t))^6 z(t)^2}.$$
Imposing that $y(t)$ satisfies the original RFDE leads to:
$$D_C^\alpha y(t) = \frac{3D_C^\alpha z(t)}{(S_C^\alpha(t))^4 z(t)} + (S_C^\alpha(t))^3 \frac{(D_C^\alpha z(t))^2}{(S_C^\alpha(t))^6 z(t)^2} + \frac{1}{(S_C^\alpha(t))^3}.$$
3. Equating the expressions and simplifying results in the second-order linear equation:
$$D_C^{2\alpha} z(t) + z(t) = 0.$$
4. Following the methods in [24] we have that the general solution for $z(t)$ is:
$$z(t) = S_C^\alpha(c_1)\cos(S_C^\alpha(t)) + S_C^\alpha(c_2)\sin(S_C^\alpha(t)).$$
5. Finally, calculating $D_C^\alpha z(t)$ and substituting back into the expression for $y(t)$, with constant $S_C^\alpha(c) = S_C^\alpha(c_2)/S_C^\alpha(c_1)$, we obtain:
$$y(t) = \frac{\sin(S_C^\alpha(t)) - c\cos(S_C^\alpha(t))}{(S_C^\alpha(t))^3(\cos(S_C^\alpha(t)) + S_C^\alpha(c)\sin(S_C^\alpha(t)))}.$$

Data availability

No data was used for the research described in the article.

References

[1] Coddington EA, Levinson N. Theory of ordinary differential equations. New York: McGraw-Hill; 1955.
[2] Verhulst F. Nonlinear differential equations and dynamical systems. Springer-Verlag; 1996.
[3] Edwards CH, Penney DE. Differential equations and boundary value problems: computing and modeling. Pearson Educación; 2000.
[4] Bellon J. Riccati equations in optimal control theory [Ph.D. thesis], Georgia State University; 2008.
[5] Martin C. Finite escape time for Riccati differential equations. Systems Control Lett 1981;1(7):127–31.
[6] Crouch PE, Pavon M. On the existence of solutions of the Riccati differential equation. Systems Control Lett 1987;9(3):203–6.
[7] Mandelbrot BB. The fractal geometry of nature. New York: W. H. Freeman; 1982.

[8] Massopust PR. Fractal functions and fractal surfaces and wavelets. Massachusetts: Academic Press; 2017.
[9] Falconer K. Fractal geometry: mathematical foundations and applications. New York: John Wiley & Sons; 2004.
[10] Feder J. Fractals. New York: Springer Science & Business Media; 2013.
[11] Kigami J. A harmonic calculus on the Sierpinski spaces. Jpn J Appl Math 1989;6(2):259–90.
[12] Kigami J. Analysis on fractals. Cambridge: Cambridge University Press; 2001.
[13] Jorgensen PET. Analysis and probability: Wavelets, signals. In: Fractals. New York: Springer Science & Business Media; 2006.
[14] Jiang H, Su W. Some fundamental results of calculus on fractal sets. Commun Nonlinear Sci Numer Simul 1998;3(1):22–6.
[15] Bongiorno D, Corrao G. An integral on a complete metric measure space. Real Anal Exch 2015;40(1):157–78.
[16] Barlow MT, Perkins EA. Brownian motion on the Sierpinski gasket. Probab Th Rel Fields 1988;79(4):543–623.
[17] Valarmathi R, Gowrisankar A. On the variable order fractional calculus of fractal interpolation functions. Fract Calc Appl Anal 2023;26(3):1273–93.
[18] Tyagi S, Martha SC. Finite-time stability for a class of fractional-order fuzzy neural networks with proportional delay. Fuzzy Sets Syst 2019.
[19] Srivastava HM, Abbas S, Tyagi S, Lassoued D. Global exponential stability of fractional-order impulsive neural network with time-varying and distributed delay. Math Methods Appl Sci 2018;41:2095–104.
[20] Parvate A, Gangal AD. Calculus on fractal subsets of real line-I: Formulation. Fractals 2009;17(01):53–81.
[21] Parvate A, Satin S, Gangal AD. Calculus on fractal curves in $\mathbb{R}^n$. Fractals 2011;19(01):15–27.
[22] Golmankhaneh AK. Fractal calculus and its applications. Singapore: World Scientific; 2022.
[23] Golmankhaneh AK, Bongiorno D. Exact solutions of some fractal differential equations. Appl Math Comput 2024;472:128633.
[24] Golmankhaneh AK, Bongiorno D. Fractal differential equations of 2 α-order. Axioms 2024;13(11):786.
[25] Golmankhaneh AK, Bongiorno D. On homogeneous system of fractal differential equations. J Math Sci 2025.
[26] Golmankhaneh AK, Bongiorno D, Ramazanova AT. Fractal calculus: nonhomogeneous linear systems. J Nonlinear, Complex Data Sci 2025.
[27] Uc M. Spectral and algebraic analysis of the fractal Volterra operator on $C^k(F)$, chaos. Solitons & Fractals 2025;200:117061.
[28] Mattila P. Geometry of sets and measures in Euclidean spaces: fractals and rectifiability. Cambridge University Press; 1995.
[29] Golmankhaneh AK, Zayed AI, Myrzakulov R. Solving fractal differential equation via numerical methods. Arab J Math 2025;1–8.
[30] Golmankhaneh AK, Pellis S, Zingales M. Fractal schrödinger equation: implications for fractal sets. J Phys A 2024;57(18):185201.
[31] Bagchi BK. Supersymmetry in quantum and classical mechanics. Boca Raton: Chapman & Hall/CRC; 2000.
[32] Gangopadhyaya A, Mallow JV, Rasinariu C. Supersymmetric quantum mechanics: an introduction. Singapore: World Scientific; 2017.